

Chaotic Orbit of Low Energy Charged Particles in a Compact Dipole Magnetic Field Configuration^{*)}

Haruhiko SAITOH and Itsuki TANIOKA

Graduate School of Frontier Sciences, The University of Tokyo, Kashiwa, Chiba 277-8561, Japan

(Received 20 December 2021 / Accepted 21 January 2022)

Conditions for the emergence of chaotic orbit of low energy positrons are numerically calculated in a compact dipole trap for use in positron and electron-positron plasma experiments. Due to its relatively weak field strength and existence of magnetic null line near the confinement region, coupling between gyro and bounce motions is pronounced even for low energy particles in this trapping geometry. Breakdown of first and second adiabatic invariants and the resultant non-integrable chaotic motion are realized for positrons with kinetic energy below the order of 10 eV. This kinetic energy value is two orders of magnitude smaller than the threshold value for a chaotic orbit in the Ring Trap-1 (RT-1) experiment. The stochastic long orbit is potentially applicable for efficient injection and compression schemes of positrons in a compact levitated dipole experiment.

© 2022 The Japan Society of Plasma Science and Nuclear Fusion Research

Keywords: orbit chaos, positron plasma, electron plasma, non-neutral plasma, levitated dipole experiment

DOI: 10.1585/pfr.17.2401026

1. Introduction

The dipole field is among the most basic magnetic configurations observed in space and in the laboratory [1], and has several scientific applications. As observed in the magnetosphere of Jupiter, the dipole configuration is capable of confining high- β plasma, which is suitable for burning advanced fusion fuels [2]. Experimentally, the Ring Trap-1 (RT-1) [3] and Levitated Dipole eXperiment (LDX) [4] have succeeded in stably generating high- β plasma [5] in a dipole field configuration with a levitated superconducting coil. There have been other attempts to apply the excellent confinement capability of the dipole to exotic plasmas, namely electron-positron pair plasmas [6–9]. Electron-positron plasmas exhibit unique wave and stability properties as a pair plasma consisting of equal mass particles [10], and have been subject to intensive theoretical and numerical investigations. However, this class of magnetically-confined matter-antimatter plasma has not yet been realized in the laboratory. A toroidal dipole geometry is one type of simultaneous trapping configuration for electrons and positrons. Because the available positron beam intensity is quite limited, it is not straightforward to create a high-density state of positrons satisfying plasma conditions. Development of a compact levitated dipole with a small confinement volume, efficient injection schemes, and radial compression methods is in progress [8].

For the creation of dense positron and electron-positron plasmas in a dipole field, efficient transport of injected positrons into the strong field region is needed. The

nature of inward (or up-hill) particle diffusion [1] of the strongly inhomogeneous dipole configuration is a promising effect for this purpose. Also, application of so-called rotating wall (RW) type electric fields for particle compression in the dipole field geometry has been discussed [11]. However, because such radial transport motions couple with the toroidal circulation motion of particles, they are rather slow processes. When injected particles have regular motion, they are typically immediately lost at the injection port structure after making one toroidal circulation and before the compression effects take place. Here chaotic motion of particles is attractive because particles with stochastic motion at the edge of a trap may have longer lifetimes that are comparable to the time scale of the slow radial compression process.

In our previous study in the relatively strong magnetic field of RT-1 (dipole field coil radius $r_{sc} = 25$ cm and current $I_{sc} = 250$ kA), we found that chaotic effects take place because of the breakdown of the first and second adiabatic invariants for electrons and positrons with kinetic energies of typically more than 10 keV [12]. Although such chaotic behavior and longer flight length was successfully verified by using high energy positrons supplied from a Na-22 source (endpoint kinetic energy is 543 keV), it is difficult to use such high energy particles for trapping and plasma experiments. Here, the planned compact levitated dipole trap for pair-plasma experiments has a superconducting coil with a much smaller magnetic moment and a magnetic field null line closer to the confinement region. These effects may enhance the occurrence of chaos of the charged particle orbit with lower kinetic energy compared to RT-1, making it potentially applicable for the efficient injection and radial compression of particles in pair-plasma

author's e-mail: saito@ppl.k.u-tokyo.ac.jp

^{*)} This article is based on the presentation at the 30th International Toki Conference on Plasma and Fusion Research (ITC30).

experiments. In this study, we numerically access the conditions for the occurrence of orbit chaos of positrons in the planned trap according to the machine parameters.

2. Numerical Trace of Positron Orbit in a Dipole Magnetic Field Trap

We calculate the regular and chaotic behavior of positron orbit in the geometry of the compact dipole experiment shown in Fig. 1. A superconducting (SC) dipole field coil can be magnetically levitated by using the feedback-controlled levitation coil magnet located above the confinement region. A mechanically supported state of the SC coil, possibly with DC bias, is another possible operation method at least for positron injection experiments [6, 7]. As coil parameters, we choose a radius $r_{sc} = 5$ cm and current $I_{sc} = 10$ kA unless otherwise specified. The trap system is surrounded by toroidally separated outer wall electrodes for the application of RW type electric fields, which are beyond the scope of the present study. The relativistic equation of motion in electromagnetic fields \mathbf{E} and \mathbf{B} is

$$\frac{d\mathbf{x}}{dt} = \mathbf{v} = \frac{\mathbf{u}}{\gamma} \quad \text{and} \quad \frac{d\mathbf{u}}{dt} = \frac{q}{m} \left(\mathbf{E} + \frac{\mathbf{u}}{\gamma} \times \mathbf{B} \right), \quad (1)$$

where $\mathbf{u} = \gamma\mathbf{v}$, $\beta = v/c$, $\gamma = 1/\sqrt{1-\beta^2}$, $m = \gamma m_0$, and m_0 is the rest mass of a positron. Three adiabatic invariants, the magnetic moment μ , longitudinal invariant J , and magnetic flux Ψ , are defined as actions for these periodic motions and are calculated according to

$$\mu = \int \frac{\gamma^2 v_{\perp}^2}{B} dt, \quad J = \int \gamma v_{\parallel} ds, \quad \Psi = \int \mathbf{B} \cdot d\mathbf{S}. \quad (2)$$

Although we use equations similar to those used for orbit chaos analysis in RT-1 [12], in this study we take advantage of the Buneman-Boris (BB) algorithm for weakly relativistic particles [13], which allows us to make stable longer-time integration. We solve the differentiated equations

$$\frac{\mathbf{x}^{n+1} - \mathbf{x}^n}{\Delta t} = \frac{\mathbf{u}^{n+1/2}}{\gamma^{n+1/2}} \quad \text{and}, \quad (3)$$

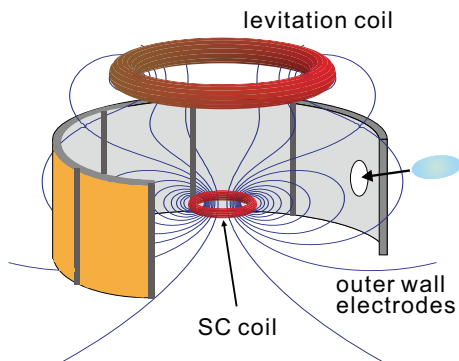


Fig. 1 Geometry of compact levitated dipole experiment. Thin lines show magnetic field lines generated by superconducting (SC) and levitation coils.

$$\frac{\mathbf{u}^{n+1/2} - \mathbf{u}^{n-1/2}}{\Delta t} = \frac{q}{m} \left(\mathbf{E}^n + \frac{\mathbf{u}^{n+1/2} + \mathbf{u}^{n-1/2}}{2\gamma^n} \times \mathbf{B}^n \right), \quad (4)$$

in a Cartesian coordinate. By introducing

$$\mathbf{u}^- = \mathbf{u}^{n-1/2} + \frac{q}{m} \mathbf{E}^n \frac{\Delta t}{2}, \quad \mathbf{u}^+ = \mathbf{u}^{n+1/2} - \frac{q}{m} \mathbf{E}^n \frac{\Delta t}{2}, \quad (5)$$

we have

$$\frac{\mathbf{u}^+ - \mathbf{u}^-}{\Delta t} = \frac{q}{2\gamma^n m} (\mathbf{u}^+ + \mathbf{u}^-) \times \mathbf{B}^n. \quad (6)$$

Then \mathbf{u}^+ is calculated in two steps as

$$\mathbf{u}^* = \mathbf{u}^- + \mathbf{u}^+ \times \frac{q\mathbf{B}^n}{2m\gamma^n} \Delta t, \quad \mathbf{u}^+ = \mathbf{u}^- + \mathbf{u}^* \frac{2\mathbf{T}}{1+T^2}, \quad (7)$$

and the next step values are given by

$$\mathbf{u}^{n+1/2} = \mathbf{u}^+ + \frac{q}{m} \mathbf{E}^n \frac{\Delta t}{2}, \quad \mathbf{x}^{n+1} = \mathbf{x}^n + \frac{\mathbf{u}^{n+1/2}}{\gamma^{n+1/2}} \Delta t. \quad (8)$$

In the following calculations, we use external magnetic fields generated by ring currents and do not include the effects of electric fields. Figure 2 shows a comparison of the stability of calculated orbit in a dipole field obtained by the 4th order Runge-Kutta (RK) and BB methods. These are evaluated by plotting the spatial error of orbit defined as

$$r_{\text{err}}(t) = |r_{\text{min}}(t) - r_{\text{min_ini}}| + |r_{\text{max}}(t) - r_{\text{max_ini}}|, \quad (9)$$

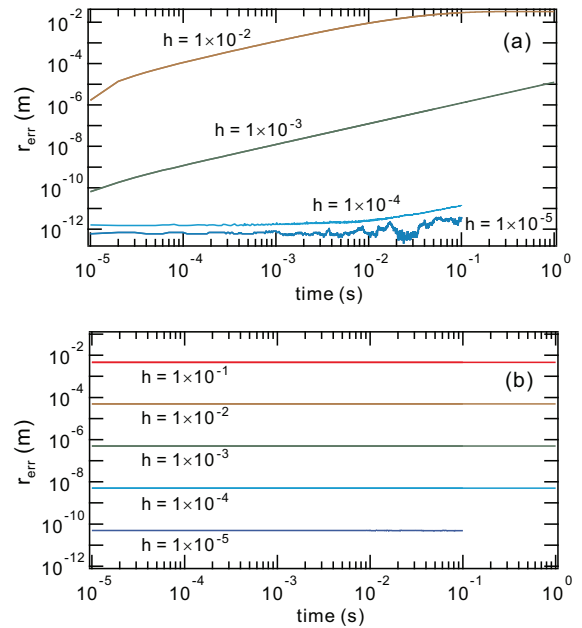


Fig. 2 Temporal evolution of r_{err} in (9) calculated by the (a) Runge-Kutta and (b) Buneman-Boris methods for different time step h normalized by gyro period.

for different time step h for a calculation period up to 1 s, where h is normalized by the gyro period. Here r_{\min} and r_{\max} are the minimum and maximum distances, respectively, from the center axis of the dipole trap in one gyromotion of particle, and r_{\min_ini} and r_{\max_ini} are their initial values, respectively. While calculation error in the spatial position is temporally accumulated in RK, BB is stable and shows no substantial growth of error for various h values. The long-term integration of positron orbit with spatial accuracy of the order of μm is obtained in realistically short calculation time in the present geometry.

3. Emergence of Chaotic Orbit and Parameter Dependence

Figure 3 shows examples of regular and chaotic orbits of positrons in a dipole field configuration (typical cyclotron radius is 1 cm for 10 eV and 3 cm for 100 eV). It is well known that the orbit of a low energy charged particle in the dipole field consists of gyration, bounce, and toroidal circulation motions. Here, toroidal circulation is realized by the grad-B and curvature drifts in the inhomogeneous dipole field. Conservation of adiabatic invariants ensures the excellent confinement properties of particles on the magnetic surfaces in the dipole geometry [2]. Adiabaticity is not always the case because of the breakdown of the constant nature of μ , J , and Ψ for various reasons. While cross-field transport driven by so-called low-frequency fluctuations plays an essential role through the selective breakdown of Ψ [1], there is another mechanism of chaos in a toroidally symmetric geometry. For particles with considerable kinetic energy, nonlinear coupling between gyro and bounce motions breaks the conservation of μ and J [14]. As particle motion has only two conserved quantities in this case, namely Ψ and kinetic energy K in a three-dimensional Hamiltonian system, the particle orbit is, in general, non-integrable and potentially

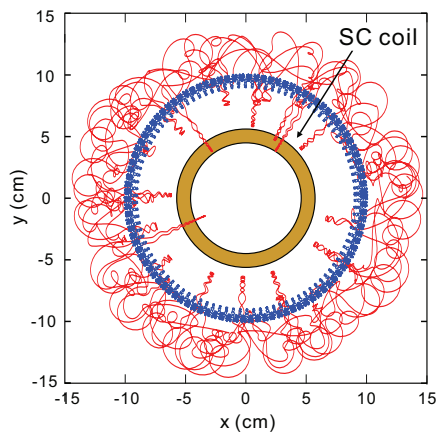


Fig. 3 Typical periodic (blue, $K = 10\text{ eV}$) and stochastic (red, $K = 100\text{ eV}$) motions of positron trapped in a dipole magnetic field, as a top view of the trap configuration.

chaotic [15, 16].

Figure 4 shows the r - V_r Poincaré section ($z = 0$) of a positron with a marginal kinetic energy K for the emergence of chaotic motion. The variation of nonintegrability is found by changing the pitch angle θ of positron injection against the magnetic field. The adiabaticity of a particle with small pitch angle is easily broken because these particles feel large field variation on the trajectories. As shown in the Fig. 4, while orbit is quasi-periodic (outermost chain line) for $\theta = 90^\circ$, chaotic trajectories cover almost the entire allowed region of the phase space for smaller θ values. Due to the conservation of two quantities, K and Ψ , particle orbit in the phase space is limited inside a finite region.

From a practical viewpoint, injected positrons with regular orbits are lost in a short time, most likely at the mechanical structure of the injection port after making just one toroidal circulation (blue line in Fig. 3). These positrons may not have the long flight length required for efficient radial compression. On the other hand, positrons with chaotic orbits (red line in Fig. 3) can stochastically have longer flight length before annihilation, without hitting the injection structure, during several toroidal circulations [12]. Because such a chaotic orbit is caused by the breakdown of adiabatic invariants in an asymmetric system, we use the temporal variation of μ as a measure of chaotic nature. Figure 5 plots the temporal evolution of μ normalized by $\bar{\mu}$, the time-averaged value of μ in the calculation period. Here μ shows large temporal variation when the particle travels in a weaker field region. When the orbit is traced for $100\ \mu\text{s}$, we found that the threshold value for the completely chaotic orbit (i.e., points in the Poincaré plot fill almost the entire allowed region) is $\alpha = (\mu_{\max} - \mu_{\min})/\bar{\mu} \sim 50\%$.

Figure 6 plots the above defined α for a flight time of $100\ \mu\text{s}$ for the various kinetic energy values, K , and pitch angle values, θ , of a positron when injected from the equator of the dipole field with different radial positions. The magnetic field is generated solely by the SC coil located

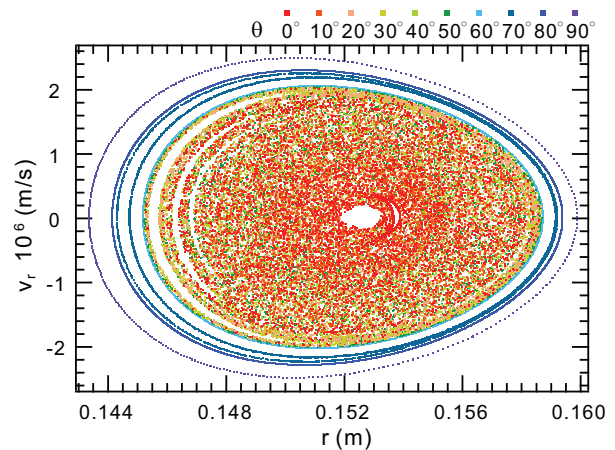


Fig. 4 Poincaré plot of particles injected from the equator of the dipole field trap with 10 different injection pitch angles.

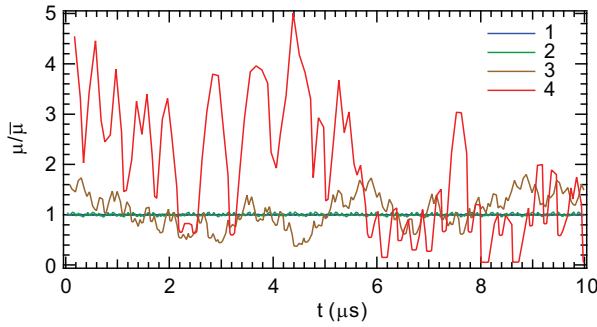


Fig. 5 Temporal variation of μ of positron orbit started from the equator with radial position r of (1) 10, (2) 15, (3) 20, and (4) 25 cm in a dipole field generated by 10 kA of ring current with a radius of 5 cm.

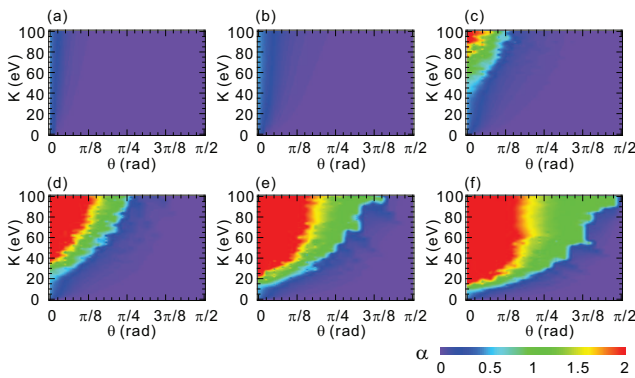


Fig. 6 Contour plot of $\alpha = (\mu_{\max} - \mu_{\min})/\bar{\mu}$ of positrons in a pure dipole field when injected from radial position, r , of (a) 7.5, (b) 10, (c) 12.5, (d) 15, (e) 17.5, and (f) 20 cm on the equator.

on the $z = 0$ plane with a total current of 10 kA and center radius of 5 cm (see Fig. 7 (1a) for the shape of the magnetic surfaces). In marked contrast to the case of the high-field dipole trap of RT-1, chaotic orbit appears for the order of $K = 10$ eV when injected with small pitch angles. As anticipated in Fig. 3, positrons in these chaotic orbits are still magnetized by the dipole field and make circulation motion around the SC coil.

Finally, the effects of the additional current of a levitation coil, located at $z = 10$ cm, with a radius of $r_{\text{lev}} = 10$ cm is shown in Fig. 7. Positron orbits are traced from the start point of $r = 10$ cm on the equator (denoted by “x” in the figure) in separatrix configurations. Existence of the magnetic null line near the trap region greatly enhances the chaotic behavior of the positron orbit. When the start position is very close to the separatrix, as shown in Fig. 7 (f), positrons above several eV of K exhibit stochastic motion. These results confirm the emergence of the chaotic behavior of low-energy positrons when injected from the edge confinement region for realistic coil and injection parameters.

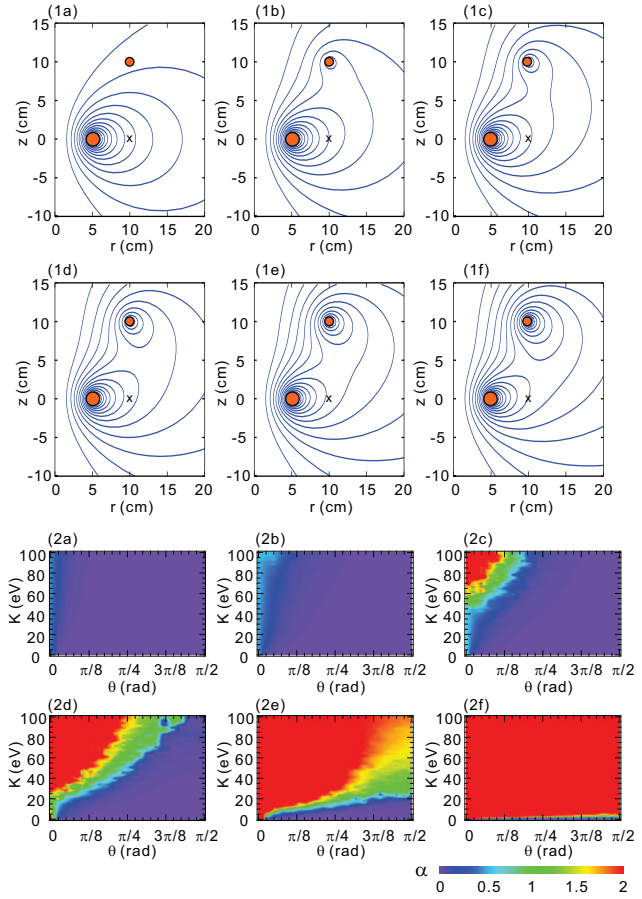


Fig. 7 (1) Magnetic field lines generated by the SC and levitation coils (located at the orange circles) and (2) contour plots of α for different levitation coil currents, I_{lev} , of (a) 0, (b) 1, (c) 1.5, (d) 2, (e) 2.5, and (f) 3 kA, while keeping an SC coil current of $I_{\text{sc}} = 10$ kA.

4. Summary

We numerically traced positron trajectories for typical parameters of a compact levitated dipole experiment to access the orbit chaos caused by the breakdown of adiabatic invariants in an asymmetric system. It is shown that gyro and bounce motion coupling is pronounced for lower energy charged particles, on the order of 10 eV, in the compact geometry. This is in marked contrast to the case of RT-1, where keV-order kinetic energy is required for the emergence of chaotic motion for positrons and electrons. Considerably lower magnetic field strength and the existence of the magnetic null line close to the confinement region are major reasons for this difference. Because chaotic particles may have long flight lengths before annihilation on the mechanical structure [12], such effects are potentially applicable for the future study of efficient positron injection and compression schemes into a dipole field.

This work was supported by NIFS Collaboration Research Program No. NIFS21KECA093.

[1] Z. Yoshida, H. Saitoh, Y. Yano, H. Mikami, N. Kasaoka *et al.*, Plasma Phys. Control. Fusion **55**, 014018 (2013).

- [2] A. Hasegawa, *Com. Plasma Phys. Cntrl. Fusion* **11**, 147 (1987).
- [3] Z. Yoshida, Y. Ogawa, J. Morikawa, S. Watanabe and Y. Yano *et al.*, *Plasma Fusion Res.* **1**, 008 (2006).
- [4] A.C. Boxer, R. Bergmann, J.L. Ellsworth, D.T. Garnier, J. Kesner *et al.*, *Nat. Phys.* **3**, 207 (2010).
- [5] M. Nishiura, Z. Yoshida, H. Saitoh, Y. Yano, Y. Kawazura *et al.*, *Nucl. Fusion* **55**, 053019 (2015).
- [6] E.V. Stenson, S. Nissl, U. Hergenbahn, J. Horn-Stanja, M. Singer *et al.*, *Phys. Rev. Lett.* **121**, 235005 (2018).
- [7] J. Horn-Stanja, S. Nissl, U. Hergenbahn, T. Sunn Pedersen, H. Saitoh *et al.*, *Phys. Rev. Lett.* **121**, 235003 (2018).
- [8] M.R. Stoneking, T. Sunn Pedersen, P. Helander, H. Chen, U. Hergenbahn *et al.*, *J. Plasma Phys.* **86**, 155860601 (2020).
- [9] H. Higaki, C. Kaga, K. Fukushima, H. Okamoto, Y. Nagata *et al.*, *New J. Phys.* **19**, 023016 (2017).
- [10] E.V. Stenson, J. Horn-Stanja, M.R. Stoneking and T. Sunn Pedersen, *J. Plasma Phys.* **83**, 595830106 (2017).
- [11] H. Saitoh, J. Horn-Stanja, S. Nissl, E.V. Stenson, U. Hergenbahn *et al.*, *AIP Conf. Procs.* **1928**, 020013 (2018).
- [12] H. Saitoh, Z. Yoshida, Y. Yano, M. Nishiura, Y. Kawazura *et al.*, *Phys. Rev. E* **94**, 043203 (2016).
- [13] H. Qin, S. Zhang, J. Xiao, J. Liu, Y. Sun and W.M. Tang, *Phys. Plasmas* **20**, 084503 (2013).
- [14] S. Murakami, T. Sato and A. Hasegawa, *Phys. Fluids B* **2**, 715 (1990).
- [15] Y. Xie and S. Liu, *Chaos* **30**, 123108 (2020).
- [16] J. von der Linden, G. Fiksel, J. Peebles, M.R. Edwards, L. Willingale *et al.*, *Phys. Plasmas* **28**, 092508 (2021).